

20. Spectral Properties of Some Weak Electron-Donor-Acceptor (EDA)-Complexes in the Far Infrared (FIR.) Region (40–400 cm^{-1})

by Michel Rossi¹⁾ and Edwin Haselbach

Physikalisch-chemisches Institut der Universität Basel, Klingelbergstrasse 80, CH-4058 Basel

(25.X.78)

Summary

The absorption spectra of 11 solid-state EDA-complexes of unsaturated hydrocarbon donors with TCNE as acceptor have been studied in the FIR. region (40–400 cm^{-1}). The dominant feature in the spectra is the appearance of a new intense absorption in the region 80–100 cm^{-1} which is assigned to the intra charge-transfer lattice mode. The (idealized) force constant for this lattice mode is found to be roughly constant for most of the EDA-complexes and is thus believed to be a measure of the total interaction of donor and acceptor within the crystal site. Force constants differing in magnitude from those of the majority of complexes are traced back to a particular structure of the donor component and/or the EDA-crystal as a whole. A recently proposed reassignment of the *Raman* active fundamentals of pure TCNE is questioned in view of the present findings.

1. Introduction. – In the course of many cycloaddition reactions long wavelength CT-absorptions due to transient electron donor-acceptor(EDA)-complexes are observed [1] [2]. Two possibilities are conceivable for the mechanistic role played by these species [3]:

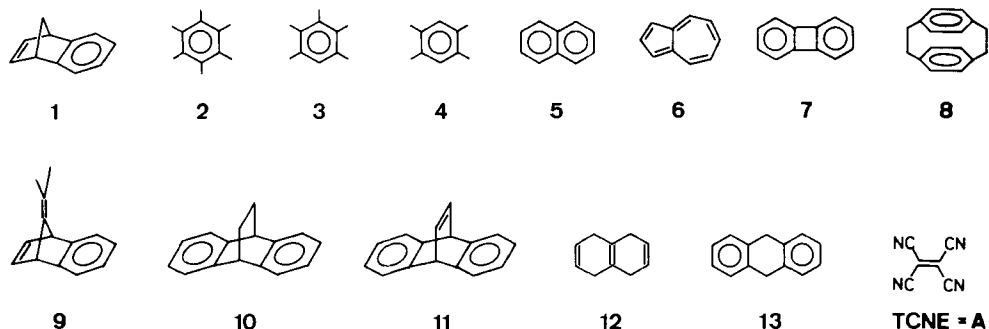
- the EDA-complex collapses to the cycloadduct and is thus a true reaction intermediate;
- the donor (**D**)/acceptor (**A**) system, at no stage of its addition process, exhibits the same nuclear configuration as the transient EDA-complex, the reaction coordinates for addition and complex formation thus differing markedly.

It follows at once that detailed information about the structure of the EDA-complex in fluid phase would enable one to make a decision in favor of one of the two alternatives. Such information, however, is somewhat controversial for non-reactive systems [4] [5] and completely lacking for reactive systems.

A methodology to approach this question was exemplified by us using the non-reactive EDA-system benzonorbornadiene (**1**) · TCNE. The olefinic moiety of **1** provides the site of attack in 'inverse electron demand' cycloadditions [6]. On the

¹⁾ Present address: Stanford Research Institute, Menlo Park, Calif. 94025, U.S.A. Correspondence should be addressed to this author.

other hand, complexation with TCNE takes place at the benzene moiety of **1** as evidenced by a comparative study of the PE. spectrum of **1** [7] and the electronic spectrum of the EDA-complex [8]. Further support for this conclusion was obtained from IR. and FIR. studies of the complex [8]. The agreement between the various observations initiated the present study of FIR. spectra of other weakly bonded EDA-systems in the crystalline state with **A**=TCNE, aimed at obtaining insight as to where and to what extent interaction between **D** and **A** occurs.



2. Preliminaries. – 2.1. *The structure of EDA-complexes from X-ray diffraction.* X-ray structural information is available only for two out of the 11 presently studied crystalline complexes.

2.1.1. *Hexamethylbenzene (2) · TCNE ((1:1)-complex)* [9]. Triclinic crystals: $C_{12}H_{18} \cdot C_6N_4$, $P\bar{1} - C_i^1$, 1 formula unit per conventional unit-cell and *Bravais*-cell. **2** and TCNE both occupy crystal sites of C_i -symmetry, which are not equivalent. **DADA** ... stacks along needle axis *c* (= body diagonal of triclinic cell).

2.1.2. *Naphthalene (5) · TCNE* [10]. Monoclinic crystals: $C_{10}H_8 \cdot C_6N_4$, $C2/m - C_{2h}^3$, 2 formula units per conventional unit-cell, 1 formula unit per *Bravais*-cell. Naphthalene and TCNE both occupy crystal sites of C_{2h} -symmetry, which are not equivalent. **DADA** ... stacks parallel to *c*.

2.2. *Selection rules.* With the above structural information the selection rules for IR. and *Raman* activity were derived according to the correlation method [11]. *Tables 1-3* show the symmetry correlation diagrams and *Tables 4* and *5* the results of the factor group analysis for the EDA-complexes **2** · **A** and **5** · **A** under the constraint of $k=0$. This means that all unit-cells vibrate against each other in phase or nearly so. From *Table 4* it can be seen, that for the (1:1)-complex **2** · **A** three IR. active translatory lattice modes ($3 \cdot a_u$) can be expected. In the case of the (2:1)-complex **2** · **2** · **A** hexamethylbenzene most probably will occupy C_1 -sites whereas TCNE will remain in C_i -sites [12]. In this case six IR. active translatory modes ($6 \cdot a_u$) are to be expected together with nine *Raman* active rotatory lattice modes ($9 \cdot a_g$). Despite the different X-ray diffraction structures of pure [2.2]-*p*-cyclophane [13] and [3.3]-*p*-cyclophane [14], it is probable that the EDA-complex **8** · **A** will have the same crystal structure as [3.3]-*p*-cyclophane · TCNE, namely $P\bar{1} - C_i^1$ [15]. In this case *Table 4* indicates that three IR. active lattice vibrations ($3 \cdot a_u$) are to be expected for **8** · **A**.

Table 1. Correlation diagram for TCNE(A)

Factor group	Site group	Point group	Site group	Factor group
C_i^I	C_i	$C_2(x)$ D_{2h}	C_2 C_{2h}	C_{2h}^3
$a_g(Ra)$	$a_g(Ra)$	$\left\{ \begin{array}{l} a_g(Ra) \\ b_{1g}(Ra) \\ b_{2g}(Ra) \\ b_{3g}(Ra) \end{array} \right.$	$\left\{ \begin{array}{l} a_g(Ra) \\ b_g(Ra) \end{array} \right.$	$\left\{ \begin{array}{l} a_g(Ra) \\ b_g(Ra) \end{array} \right.$
$a_u(IR.)$	$a_u(IR.)$	$\left\{ \begin{array}{l} a_u \\ b_{1u}(IR.) \\ b_{2u}(IR.) \\ b_{3u}(IR.) \end{array} \right.$	$\left\{ \begin{array}{l} a_u(IR.) \\ b_u(IR.) \end{array} \right.$	$\left\{ \begin{array}{l} a_u(IR.) \\ b_u(IR.) \end{array} \right.$

Table 2. Correlation diagram for hexamethylbenzene (2)

Point group	Site group	Factor group
D_{6h}	C_i	C_i^I
$\left\{ \begin{array}{l} a_{1g}(Ra), a_{2g} \\ b_{1g}, b_{2g} \\ e_{1g}(Ra), e_{2g}(Ra) \end{array} \right.$	$a_g(Ra)$	$a_g(Ra)$
$\left\{ \begin{array}{l} a_{1u}, a_{2u}(IR.) \\ b_{1u}, b_{2u} \\ e_{1u}(IR.), e_{2u} \end{array} \right.$	$a_u(IR.)$	$a_u(IR.)$

Table 3. Correlation diagram for naphthalene (5)

Point group	Site group	Factor group
$C_2(x)$	C_2	
D_{2h}	C_{2h}	C_{2h}^3
$\left\{ \begin{array}{l} a_g(Ra) \\ b_{1g}(Ra) \\ b_{2g}(Ra) \\ b_{3g}(Ra) \end{array} \right.$	$\left\{ \begin{array}{l} a_g(Ra) \\ b_g(Ra) \end{array} \right.$	$\left\{ \begin{array}{l} a_g(Ra) \\ a_g(Ra) \end{array} \right.$
$\left\{ \begin{array}{l} a_u \\ b_{1u}(IR.) \\ b_{2u}(IR.) \\ b_{3u}(IR.) \end{array} \right.$	$\left\{ \begin{array}{l} a_u(IR.) \\ b_u(IR.) \end{array} \right.$	$\left\{ \begin{array}{l} a_u(IR.) \\ a_u(IR.) \end{array} \right.$

Table 4. Selection rules for $2 \cdot A$

$P\bar{I}-C_i^I$	Factor group analysis				Activity
	$\Sigma \eta_i^a)$	$T^{(b)}$	$T^{(c)}$	$R^{(d)}$	
a_g	6	0	0	6	Ra
a_u	6	3	3	0	IR.

^{a)} $\Sigma \eta_i$: Total number of external degrees of freedom ^{c)} T: Translatory modes
^{b)} T': Number of acoustic modes ^{d)} R: Rotatory modes
 No factor group splitting for site symmetry C_i = factor group C_i^I

Table 5. Selection rules for $5 \cdot A$

$C2/m - C_{2h}^3$	Factor group analysis ^{a)}				Activity
	$\sum \eta_i$	T'	T	R	
a_g	2	0	0	2	Ra
b_g	4	0	0	4	Ra
a_u	2	1	1	0	IR.
b_u	4	2	2	0	IR.

^{a)} For explanation of symbols see Table 4.No factor group splitting for site symmetry C_{2h} = factor group C_{2h}^3 .

3. Results. - The FIR. spectra are displayed in Figures 1-4 with the corresponding results listed in Table 6. The resolution of the spectra is 7 cm^{-1} , the accuracy is believed to be $\pm 2.4 \text{ cm}^{-1}$. The spectra were obtained by conventional powder methods (finely pulverized crystals embedded in a transparent medium) and the

Table 6. FIR. transitions ($40\text{--}400 \text{ cm}^{-1}$) of pure TCNE (A) and of the solid EDA-complexes $2 \cdot A - 12 \cdot A$ (Spectra measured at room temperature)

		TCNE(A)	$2 \cdot A$	$3 \cdot A$	$4 \cdot A$	$5 \cdot A$	$6 \cdot A$
Lattice modes		85ww	71sh	68w	50ww	60ww	59-66w
		95ww	89m	$\sim 95m$, br.	68ww	65-70ww	76-78sh
					95m	96-98m	98-100m
TCNE ^{a)}	$\left\{ \begin{array}{l} \nu_{18}(b_{2u}) \\ \nu_5(a_g) \end{array} \right.$	119m	115w	115w	115w		
		(127Ra) no		128sh	129sh	122m	124-127m
		159ss	154ss, br.	151ss	152ss	156s	142sh
	$\left\{ \begin{array}{l} \nu_{12}(b_{1u}) \end{array} \right.$	166ss	164ss, br.	166ss	159ss	166s	156ss
		180ss		176ss	178sh		164ss
			242s	220s	208m		
					212m		
				313m		361m	316s
							332w
		$7 \cdot A$	$8 \cdot A$	$9 \cdot A$	$10 \cdot A$	$11 \cdot A$	$12 \cdot A$
Lattice modes			47sh				
			66m				
		54sh	85sh				66w
		69m	95m	73m	84m	78-81m	93sh
TCNE ^{a)}	$\left\{ \begin{array}{l} \nu_{18}(b_{2u}) \\ \nu_5(a_g) \end{array} \right.$	112s ^{b)} ^{c)}	124.5 ^{b)}	106w		$\sim 104m$, br.	105-108sh
		131w		128s	125s	127s	128s
		149sh	156ss, br.	152ss	155ss	154ss	156ss
	$\left\{ \begin{array}{l} \nu_{12}(b_{1u}) \end{array} \right.$	154ss	162ss, br.	162ss	173ss	171ss	166ss
		166ss	169ss, br.	176ss			180ss
		215m	188sh				
			295s	320w	334w	359w	291s
		366m	310s	342w	354w		
		376m	391s				

ww = very weak; w = weak; m = medium; s = strong; ss = very strong; sh = shoulder; no = not observed; br. = broad

^{a)} TCNE modes: $\nu_{18} = C(CN)_2$ -rocking; $\nu_5, \nu_{12} = C(CN)_2$ -scissoring.

^{b)} Assignment uncertain.

^{c)} Perhaps internal b_{2u} -mode (IR.) occurring at 120 cm^{-1} in free TCNE [33].

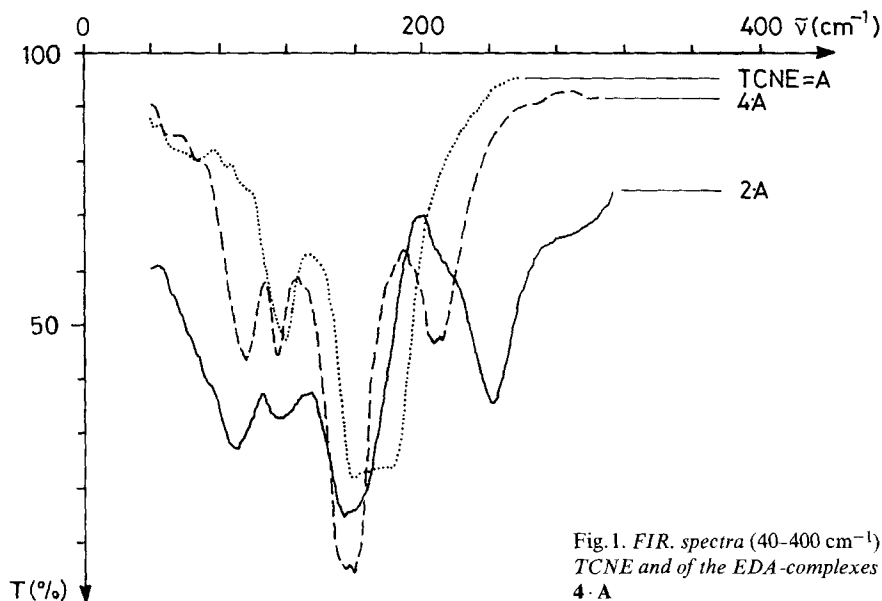


Fig. 1. FIR. spectra ($40\text{--}400\text{ cm}^{-1}$) of pure TCNE and of the EDA-complexes $2 \cdot A$ and $4 \cdot A$

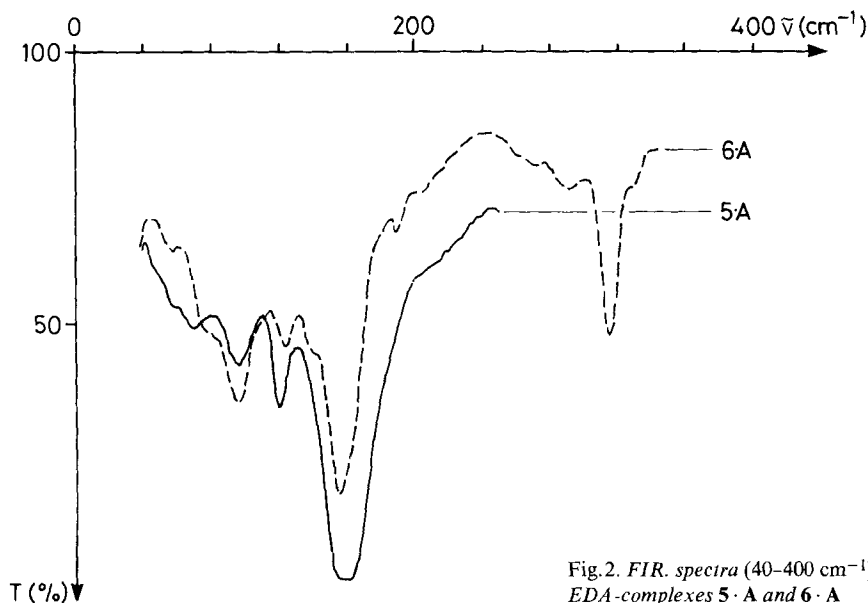


Fig. 2. FIR. spectra ($40\text{--}400\text{ cm}^{-1}$) of the EDA-complexes $5 \cdot A$ and $6 \cdot A$

polycrystalline nature of the samples was checked by X-ray diffraction (*Debye-Scherrer* method). Thereby it was found that $5 \cdot A$ and $6 \cdot A$ occurred in two different polymorphic forms according to the preparation method (see experimental section for further details). The corresponding spectra showed only minor differences in band positions and almost none in band intensities; thus, for some bands, ranges of absorption energy rather than single values are given in *Table 6*. The same was also

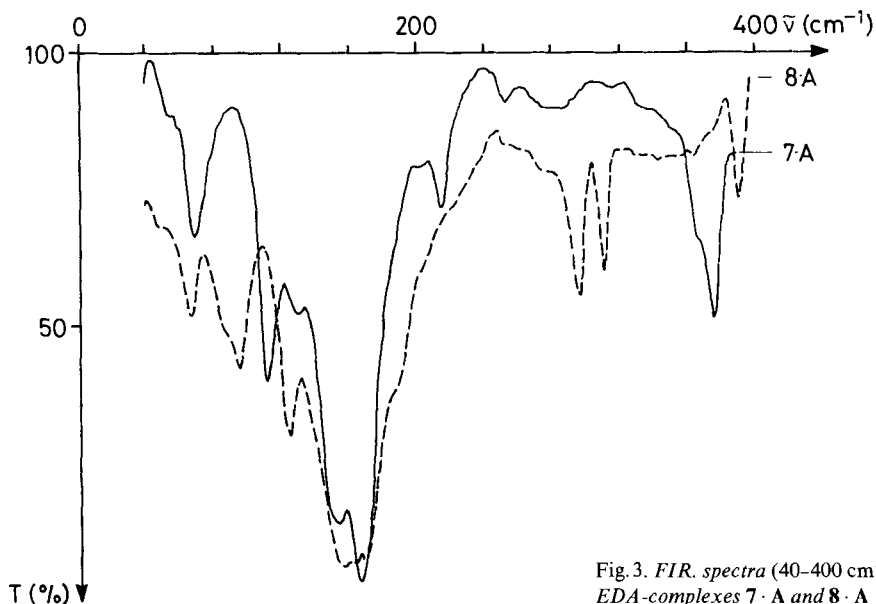


Fig. 3. FIR. spectra (40–400 cm^{-1}) of the EDA-complexes $7 \cdot A$ and $8 \cdot A$

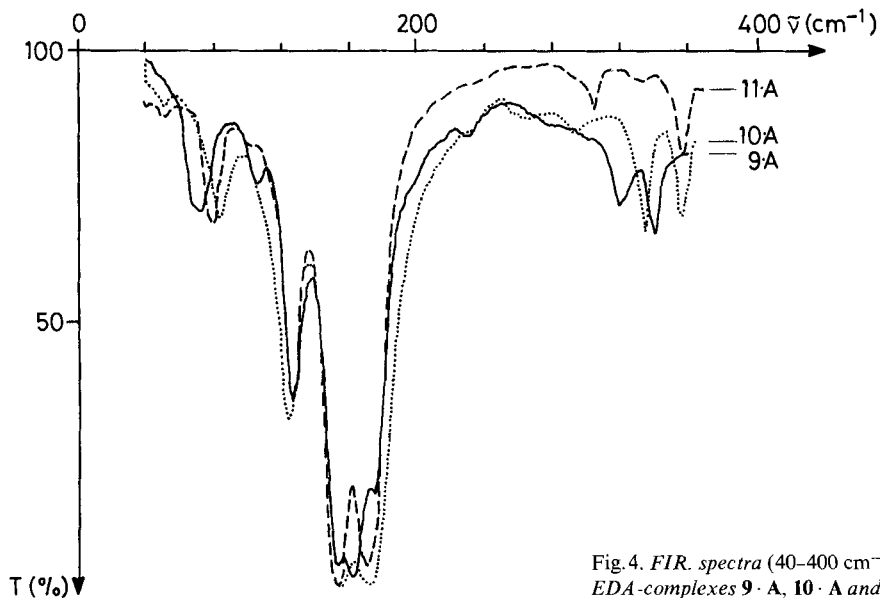


Fig. 4. FIR. spectra (40–400 cm^{-1}) of the EDA-complexes $9 \cdot A$, $10 \cdot A$ and $11 \cdot A$

found for the (1:1)- and (2:1)-complex of **2** with **A**; the band positions given in *Table 6* are those of the (2:1)-complex.

Every spectrum is the result of three or more independent recordings using different polycrystalline samples. Very weak features in the spectra (mainly lattice modes, 40–80 cm^{-1}) which were not reproducible, are not included in *Table 6*. Polymorphism of some samples or differences in crystallite size and shape could explain

these non-reproducibilities. Such phenomena are frequently encountered and well documented for FIR spectra of ionic crystals [6]. Therefore, attention should focus mainly on the more intense transitions.

4. Discussion. – The great majority of the hitherto studied organic EDA-complexes of defined stoichiometry in the crystalline phase occur in an arrangement of mixed stacks of donor and acceptor molecules [17]. In EDA-complexes there are two conceptually different kinds of lattice motions in the low frequency region: 1) phonons and 2) intra charge-transfer modes. A phonon mode consists of the displacement of the **DA**-unit as a whole. In these modes the donor and the corresponding acceptor move in phase to retain their relative geometry. An intra charge-transfer mode is an internal mode of the **DA**-unit and involves the relative displacement of the donor and acceptor within this unit. For a lattice consisting of a number n of (1:1)-complex units per unit cell with significant factor group interactions, there are $6n-3$ optical phonons, $6n$ intra charge-transfer modes and 3 acoustical phonons. It is evident, however, that the available experimental data on the lattice modes allow only a classification with respect to their symmetry species rather than an assignment to group 1) or 2) above.

Inspection of *Tables 4–6* reveals that in the case of **5 · A** all three IR. active lattice modes could be found. For **2 · A**, however, only two of the three modes (or six in the case of the (2:1)-complex listed in *Table 6*) were detected. In the absence of any structural data for the remaining EDA-complexes in *Table 6* it was impossible to determine the number and the spectral activity of the observed lattice modes.

The main feature in the lattice mode region is the occurrence of an intense absorption around $80\text{--}100\text{ cm}^{-1}$ throughout the whole series of studied EDA-complexes, with the exception of **12 · A**, which shows only weak absorptions in that range. One of the six intra charge-transfer modes ($n=1$) apparently generates a large variation in the ground state dipole moment $\vec{\mu}_N$ of the EDA-complex and therefore gives rise to this high intensity transition. We propose that this transition (underlined in *Table 6*) originates from the oscillation of the interplanar distance between **D** and **A** within the stacks.

Let us consider a one-dimensional model for the structure of a solid state EDA-complex. In such an approximation the donor and acceptor molecules are replaced by atoms in a diatomic linear lattice with coupling parallel to the stack axis and without coupling between the different stacks. The frequency for the optical branches of a diatomic linear lattice in the limit $kd_{\pi\pi} \ll 1$ ($d_{\pi\pi}$ is the lattice constant or interplanar distance in the complex crystal structure, and k is the wave vector) is given by:

$$\nu^2 = \frac{1}{4\pi^2} \omega^2 = \frac{C}{2\pi^2} \left(\frac{1}{M_1} + \frac{1}{M_2} \right). \quad (2)$$

C is the force constant, M_1 and M_2 are the atomic (or corresponding molecular) masses which make up the diatomic linear lattice [18]. In the present series one 'atomic' mass, *i.e.* the molecular mass of TCNE (M_1) is kept constant, so that a plot of ν^2 against the reciprocal of the mass of the donor (M_2) should yield a straight line

with slope $C/2\pi^2$ and intercept $C/2\pi^2 M_1$ if the force constant is roughly the same for the whole series. *Figure 5* displays such a plot (for $\tilde{\nu}^2$), indicating that most of the solid EDA-complexes (donors **2**, **3**, **4**, **5**, **6**, **10** and **11**) have about the same force constant. The usual interplanar distance for π - π molecular complexes is about 330 pm [17] (335 pm for **2** · A [9] and 330 pm for **5** · A [10]) so that the above result indicates a constant interaction of the donor with the acceptor within the stack. The charge-transfer interaction is thereby thought to constitute only a fraction of the total donor-acceptor interaction in the crystal site. It is interesting to note that the total interaction of electron donor and acceptor in the crystal is about the same for both alkylated (**2**, **3**, **4**, **10** and **11**) and annelated (**5** and **6**) aromatic hydrocarbons. This situation is not found in solution, where the total interaction between electron donor and acceptor as measured by ΔH^0 for EDA-complex formation is larger in the case of the polymethylated aromatics [19] than for naphthalene [20]. That the specific charge-transfer interaction alone does not control the magnitude of the force constant in crystalline EDA-complexes is indicated by the fact, that the isomeric complexes **5** · A and **6** · A exhibit roughly the same force constants, whereas their lowest CT. transition energies differ markedly [21].

There are, however, two crystalline EDA-complexes, whose intra charge-transfer force constants are either significantly higher (**8** · A) or lower (**7** · A) than the value obtained for the remainder of the series. One of several reasons for this observation may be that the structures of these EDA-complexes in the solid state are different from those usually observed. It is worth noting that the non-planar aromatic hydrocarbons **10** and **11** form stable EDA-complexes with TCNE, whose force constants fit the linear relation displayed in *Figure 5*, whereas in the case of **8** · A a shorter interplanar distance of 320 pm could be realized similar to the one found for [3.3]-*p*-cyclophane · TCNE [15], which would explain the larger force constant for this complex. The somewhat lower force constant in the case of **9** · A could be ascribed to steric hindrance of TCNE by the exocyclic double bond of **9**. The much lower force

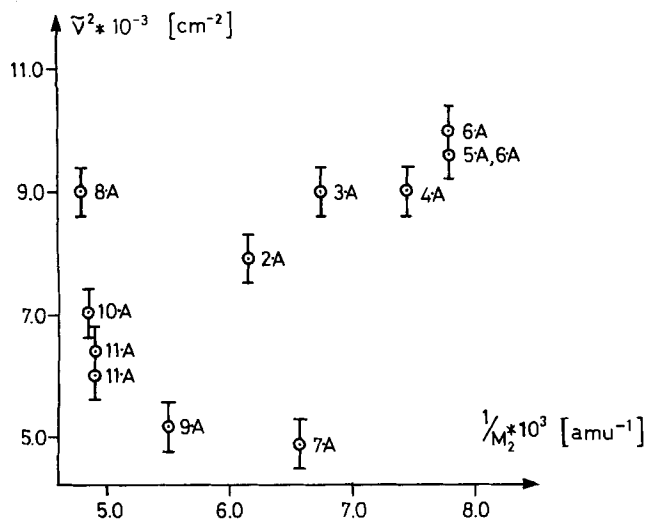


Fig. 5. Idealized one-dimensional lattice model for the EDA-complexes: Plot of $\tilde{\nu}^2$ against the reciprocal of the donor mass M_2 (see text)

constant for $7 \cdot A$ cannot be explained until X-ray crystallographic measurements of its solid state structure are available. It is, however, noteworthy that **7** has a structure intermediate between that of **5** and **13**. While $5 \cdot A$ is stable and spectroscopically behaves like an ordinary EDA-complex, any attempt to synthesize $13 \cdot A$ under a variety of conditions failed. Finally, for $12 \cdot A$ no intense FIR. absorptions around $80\text{--}100\text{ cm}^{-1}$ could be found, although other specific spectroscopic features are present (Table 6). The nature of $12 \cdot A$ is obviously very similar to that of the complex $C_{10}H_8 \cdot C_{10}F_8$ (naphthalene \cdot octafluoronaphthalene), or to that of $C_{12}H_{10} \cdot 3C_{12}H_{10}N_2O_4$ (biphenyl \cdot 3(4,4'-dinitrobiphenyl)) studied in detail by *Chen & Prasad* [22] who could find no indications of an appreciable resonance interaction. It is interesting to note that neither their complexes nor our complex $12 \cdot A$ do show a CT. transition in the UV./VIS. spectrum in solution²⁾.

With the exception of $12 \cdot A$ all other systems studied here are very similar to the complex 1,3,5-trinitrobenzene \cdot durene investigated in great detail by *Chen & Prasad* [23] using *Raman* spectroscopy. These authors reached the conclusion that charge-transfer interactions are not significantly larger than the pure crystalline interactions, a conclusion which is valid also for our EDA-complexes. Although the amount of charge-transfer may be small in terms of total donor-acceptor interaction within the crystal site, it nevertheless gives rise to the intense FIR. absorption.

It is clear that the arguments presented so far in favour of a CT. interaction in molecular crystals are somewhat qualitative in the absence of any detailed normal coordinate analysis. However, *Schrader et al.* [24] were able to identify in the case of the melamine molecular crystal a high intensity *Raman* band as pure translatory lattice mode; their careful and thorough study reveals IR. active lattice modes with a high translatory component as well. This constitutes an important result, as other workers in this field did not attribute high IR. or *Raman* intensities to these translatory lattice modes [25].

Inspection of Table 6 reveals, that $\nu_5(a_g)$ of TCNE, which is an IR. inactive (*Raman* active) symmetric scissoring mode, has little intensity in complexes of TCNE with polymethylated aromatic hydrocarbons, but large intensity in TCNE-complexes with for example the nonplanar hydrocarbons **9**, **10** and **11**. The shift as well as the activation of IR. inactive bands in EDA-complexes is an often encountered phenomenon [27] [28] and can be explained qualitatively in two ways, both yielding some information on the molecular environment of TCNE in its crystal site:

1) For EDA-complexes with small intermolecular overlap S_{01} (e.g. π, π -complexes) and small dipole moment $\vec{\mu}_0$ of the no-bond configuration $\psi(DA)$ the change in dipole moment $\vec{\mu}_N$ of the ground state EDA-complex ψ_N is given by:

$$\delta \vec{\mu}_N = 2 b \vec{\mu}_1 \delta b \quad (3)$$

²⁾ A further olefinic donor which resisted its preparation as a crystalline EDA-complex with TCNE is 3,5-cholestadiene. Again, no IR. or FIR. indications were obtained for complex formation in the solid state, though CT. interaction apparently takes place in solution as revealed by the orange-red colour of the mixture in CH_2Cl_2 .

where $\vec{\mu}_1$ is the dipole moment of the charge-transfer configuration $\psi_1(\mathbf{D}^+\mathbf{A}^-)$ and b is the mixing coefficient of $\psi_1(\mathbf{D}^+\mathbf{A}^-)$ in ψ_N .

Changes in b , which will affect $\vec{\mu}_N$ and thus cause the perturbation in intensity of a certain mode (localized either on the donor or the acceptor) can be brought about by:

(i) variation of the ionisation energy $I(\mathbf{D})$ of the donor and/or of the electron affinity $A(\mathbf{A})$ of the acceptor with the normal mode q :

$$(\delta I(\mathbf{D})/\delta q)_{q=0} \neq 0, \quad \text{and/or} \quad (\delta A(\mathbf{A})/\delta q)_{q=0} \neq 0; \quad (4)$$

(ii) variation of the intermolecular overlap S_{01} with q :

$$(\delta S_{01}/\delta q)_{q=0} \neq 0, \quad (5)$$

so that a charge oscillation between \mathbf{D} and \mathbf{A} with the normal mode q is generated. This causes a transition moment for IR. absorption perpendicular to the molecular planes. Possibility (i) is for example conceivable for the ring breathing modes of aromatic molecules, which may cause changes in ionisation energy, whereas possibility (ii) could be realized in our example $\mathbf{9} \cdot \mathbf{A}$ (Fig. 6). In $\mathbf{9} \cdot \mathbf{A}$ $\nu_5(\text{TCNE})$ changes S_{01} periodically because of steric hindrance, giving rise to an intensity enhancement of this transition in the complex.

2) The totally symmetric (*Raman* active) mode ν_5 (TCNE) is accompanied by a variation of the scalar polarizability, which leads to a periodic redistribution of valence electrons in the complex. As discussed for Na^+TCNE^- [29] this charge oscillation is the origin of a time-dependent variation of interaction between cationic and anionic centers and thus leads to

$$(\delta \vec{\mu}_N/\delta q)_{q=0} \neq 0. \quad (6)$$

This type of activation of absorption bands probably could account for the weak intensity observed for cases like $\mathbf{2} \cdot \mathbf{A}$, $\mathbf{3} \cdot \mathbf{A}$ and $\mathbf{4} \cdot \mathbf{A}$ without appreciable steric hindrance of TCNE, whereas the strong enhancement of forbidden bands in the complexes of $\mathbf{9}$, $\mathbf{10}$ and $\mathbf{11}$ is better explained by the previous steric argument.

There is no simple qualitative explanation for the splitting of the b_{1u} -band of TCNE in the solid EDA-complexes. It is unlikely that it has its origin in dynamic coupling effects, because it appears also in the spectra of $\mathbf{2} \cdot \mathbf{A}$ and $\mathbf{5} \cdot \mathbf{A}$ where X-ray crystallographic data unequivocally exclude the presence of more than one formula unit in the *Bravais*-cell.

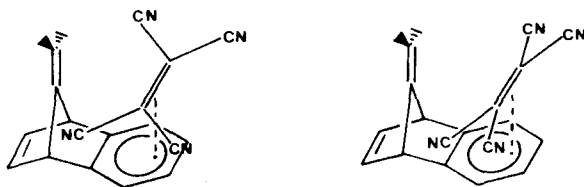


Fig. 6. Activation of the IR. inactive $\nu_5(a_g)$ mode of pure TCNE when complexed to a donor

Finally, the present work offers no support to the reassignment of the *Raman* active bands of TCNE as claimed in [30] ($\nu_5(a_g)$ at 150 cm^{-1} , a b_{2g} - or b_{1g} -mode at 130 cm^{-1}). This assignment would require a second intense absorption around 160 cm^{-1} in the FIR. spectrum of pure TCNE, *i.e.* in the vicinity of the FIR. transitions for complexed TCNE around 165 cm^{-1} as found in this work. Neither the published IR. and *Raman* spectra nor the assignment of the fundamentals [26] of pure TCNE do yield such a result.

5. Conclusions. - The following conclusions can be drawn from the present work:

1) The intra charge-transfer lattice mode of various organic donors complexed to TCNE was identified in the FIR. region around $80\text{--}100\text{ cm}^{-1}$. This mode is believed to be the oscillation of the interplanar distance between donor and acceptor within the stacks;

2) The (idealized) force constant for the translatory motion within the stack is a measure of the *total* interaction of the components in the crystal sites. This force constant is almost constant for most of the studied EDA-complexes;

3) Charge oscillations and/or periodical changes of the polarizability of the whole EDA-complex cause the activation of the $\nu_5(a_g)$ -scissoring mode of TCNE;

4) In the case of the TCNE-complex of 1,4,5,8-tetrahydronaphthalene (**12**) no specific charge-transfer interaction was found in the solid state;

5) The present results suggest that the original assignment of the *Raman* active bands of pure TCNE is correct [26] and does not need revision [30].

This work is part of project Nr. 2.544-0.76 of the «*Schweizerischer Nationalfonds zur Förderung der wissenschaftlichen Forschung*». Financial support by the «*Fonds zur Förderung von Lehre und Forschung*», Ciba-Geigy SA, F. Hoffmann-La Roche SA, Sandoz SA and Ciba-Geigy Foundation are gratefully acknowledged. We express our gratitude to Prof. H. Oswald and PD. K. Ludwig (University of Zürich) for the kind permission of using their FIR. spectrometer, to Dr. H.-R. Stieger (BBC, Baden) for invaluable advice and encouragement in interpreting the FIR. results, to Prof. St. Graeser (University of Basel) for the X-ray measurements and to Mr. U. Buser for the synthesis and purification of many compounds used in this study.

Experimental Part

The EDA-complexes were synthesized in a *Petri* disk by slow evaporation of the solvent (CH_2Cl_2 , Uvasol, Merck) from a solution of the donor and TCNE in a (1:1)- or (2:1)-ratio, or with a slight excess of the donor in cases of its high volatility. Needles up to 3 mm in size were obtained. The observed colours appeared as:

2 · A: dark brown, metallic appearance,	5 · A: red-violet, 6 · A: dark violet with purple appearance,	8 · A: reddish brown, 9 · A: dark blue,	12 · A: reddish (slightly)
3 · A: brown, 4 · A: red-brown,	7 · A: dark green,	10 · A: reddish brown, 11 · A: reddish brown,	

For the FIR. spectra a Nuyol-mull was prepared by pulverizing the crystalline EDA-complex with 2-3 drops of nuyol between two glass plates. An alternative procedure was to grind weighed amounts of the separate components between the glass plates until intense colours appeared. The microcrystalline nature of the nuyol-mull was checked in the cases of the donors **2**, **5** and **6** by

recording an X-ray diffraction spectrum in the *Debye-Scherrer* arrangement. Identical X-ray and FIR spectra were obtained for the above two methods of sample preparation. However, when the two components were ground between the glass plates without nuyol, slightly different X-ray and FIR spectra resulted. Generally, the X-ray diffraction pattern showed additional (or split) lines and the FIR absorptions were broader and/or showed minor changes in intensity.

REFERENCES

- [1] *J. Tabushi, K. Yamamura & Z. Yoshida*, J. Amer. chem. Soc. **94**, 787 (1972); *J. Tabushi, K. Yamamura, Z. Yoshida & A. Togashi*, Bull. chem. Soc. Japan **48**, 2922 (1975).
- [2] *V.D. Kiselev & J.G. Miller*, J. Amer. chem. Soc. **97**, 4036 (1976).
- [3] *R.B. Woodward*, J. Amer. chem. Soc. **64**, 3058 (1942); *J.A. Berson & W.A. Muller*, J. Amer. chem. Soc. **83**, 4940 (1961).
- [4] *J.W. Anthonsen & C.K. Moeller*, Spectrochim. Acta **33A**, 987 (1977) and references cited therein. *J.W. Anthonsen*, Spectrochim. Acta **32A**, 963 (1976).
- [5] *R.S. Mulliken & W.W. Person*, 'Molecular Complexes', Wiley Interscience, New York 1969.
- [6] *H.R. Pfändler, H. Tanida & E. Haselbach*, Helv. **57**, 383 (1974).
- [7] *E. Haselbach & M. Rossi*, Helv. **59**, 278 (1976).
- [8] *M. Rossi & E. Haselbach*, Chimia **29**, 21 (1975); *M. Rossi*, Dissertation, University of Basel 1975; *M. Rossi & E. Haselbach*, unpublished results.
- [9] *M. Saheki, H. Yamada, H. Yoshioka & K. Nakatsu*, Acta crystallogr. **32B**, 662 (1976).
- [10] *R.M. Williams & S.C. Wallwork*, Acta crystallogr. **22**, 899 (1976).
- [11] *W.G. Fateley, N.T. McDevitt & F.F. Bentley*, Appl. Spectroscopy **25**, 155 (1971).
- [12] *M. Saheki & H. Yamada*, Spectrochim. Acta **32A**, 1425 (1976).
- [13] *H. Hope, J. Bernstein & K.N. Trueblood*, Acta crystallogr. **28B**, 1733 (1972).
- [14] *P.K. Gantzel & K.N. Trueblood*, Acta crystallogr. **18**, 958 (1965).
- [15] *J. Bernstein & K.N. Trueblood*, Acta crystallogr. **B27**, 2078 (1976).
- [16] *R.W. Berg*, Spectrochim. Acta **32A**, 1747 (1976).
- [17] *C.K. Prout & B. Kamenar*, 'Crystal Structures of Electron-Donor-Acceptor Complexes' in Molecular Complexes, Vol. 1 (R. Foster, editor), Elek Science, London 1973.
- [18] *C. Kittel*, 'Introduction to Solid State Physics', 5th. ed., John Wiley, New York 1976.
- [19] *M. Rossi, U. Buser & E. Haselbach*, Helv. **59**, 1039 (1976).
- [20] *R. Foster*, in 'Molecular Complexes', Vol. I (R. Foster, editor), Elek Science, London 1973.
- [21] *R. Gschwind, E. Haselbach & M. Rossi*, unpublished work.
- [22] *F.P. Chen & P.N. Prasad*, Chem. Physics Letters **47**, 341 (1977); *B.A. Bolton & P.N. Prasad*, Chem. Physics **32**, 403 (1978).
- [23] *F.P. Chen & P.N. Prasad*, Chem. Physics **16**, 175 (1976).
- [24] *B. Schrader*, Ber. Bunsenges. phys. Chem. **78**, 1187 (1974); *J.R. Schneider & B. Schrader*, J. mol. Struct. **29**, 1 (1975).
- [25] *A. Kastler & A. Rousset*, J. Physics Rad. VIII/II, 49 (1941).
- [26] *F.A. Miller, O. Sala, P. Devlin, J. Overend, E. Lippert, W. Lueder, H. Moser & J. Varchmin*, Spectrochim. Acta **20A**, 1233 (1964); *J.H. Hinkel & J.D. Devlin*, J. chem. Physics **58**, 4850 (1973).
- [27] *E.E. Ferguson*, J. chem. Physics **61**, 257 (1964); *E.E. Ferguson & F.A. Matsen*, J. Amer. chem. Soc. **82**, 3268 (1960); *H.B. Friedrich & W.B. Person*, J. chem. Physics **44**, 2161 (1966); *H.B. Friedrich & W.B. Person*, J. chem. Physics **44**, 2161 (1966).
- [28] *J. De Leeuw & Th. Zeegers-Huyskens*, Adv. in Mol. Relax. Proc. **7**, 263 (1975); *J. De Leeuw & Th. Zeegers-Huyskens*, Bull. Soc. chim. Belg. **84**, 861 (1975).
- [29] *J.C. Moore, D. Smith, Y. Youhne & J.P. Devlin*, J. phys. Chemistry **75**, 325 (1971).
- [30] *K.H. Michaelian, K.E. Rieckhoff & E.M. Voigt*, Chem. Physics Letters **39**, 521 (1976).
- [31] *A. Girlando & C. Pecile*, J. chem. Soc. Faraday II, **69**, 818 (1973) and references therein; *B.N. Cyvin & S.J. Cyvin*, Mh. Chem. **105**, 1077 (1974); *C. Pecile & B. Lunelli*, J. chem. Physics **48**, 1336 (1965).